

# The green synthesis of xanthenedione and dihydropyrimidone derivatives catalyzed by nano-crystalline solid acid catalysts

Abbas Teimouri<sup>1\*</sup>,

Alireza Najafi Chermahini<sup>2</sup>,

Leila Ghorbanian<sup>3</sup>

<sup>1</sup> Chemistry Department,  
Payame Noor University,  
19395-4697, Tehran, I. R. of Iran

<sup>2</sup> Department of Chemistry,  
Isfahan University of Technology,  
Isfahan, 841543111, Iran

<sup>3</sup> Materials Engineering Department,  
Isfahan University of Technology,  
Isfahan, Iran

A simple highly versatile and efficient synthesis of xanthenedione and dihydropyrimidone derivatives is achieved through condensation reactions catalyst by nano-sulfated zirconia, nano-structured ZnO, nano- $\gamma$ -alumina and nano-ZSM-5 zeolites. The optical properties of the nano-structured organic molecules were studied. The advantages of methods are short reaction times and milder conditions, easy work-up and purification of products by non-chromatographic methods. The catalysts can be recovered for subsequent reactions and reused without any appreciable loss of efficiency.

**Key words:** xanthenedione, dihydropyrimidone, nano-sulfated zirconia, nanoZnO, nano- $\gamma$ -alumina, nano-ZSM-5

## INTRODUCTION

Xanthenes derivatives have attracted considerable attention to organic synthesis [1] and medicinal chemistry [2] in recent years. These compounds have been investigated for anti-inflammatory [3], antiviral [4], antimicrobial, [5] antidepressant and antimalarial [6] activities. Among them, xanthenediones form the structural unit in many of the natural product compounds [7]. Xanthenediones are synthesized by many procedures in recent years and one among the conventional methods involves acid- or base-catalyzed condensation of appropriate active methylene carbonyl compounds with aldehydes [8] since the active methylene compounds like dimedone is used as a precursor for many heterocyclic compounds [9, 10].

Various methods for the synthesis of xanthenes are described in the literature including condensation of aromatic aldehydes and dimedone using  $\text{NaHSO}_4 \cdot \text{SiO}_2$  [11],  $\text{TiO}_2/\text{SO}_4^{2-}$  [12], Dowex-50 W [13], silica sulfuric acid [14],  $\text{ZrOCl}_2 \cdot 8\text{H}_2\text{O}$  [15],  $\text{InCl}_3 \cdot 4\text{H}_2\text{O}$  [16],  $\text{FeCl}_3 \cdot 6\text{H}_2\text{O}$  [17],  $\text{Fe}^{3+}$ -montmorillonite [18]. Alumina-sulfuric acid [19] and amberlyst-15 catalyst [20] as solid acid catalysts have been proposed. In addition, the synthesis of other xanthenedione derivatives over HPWA/MCM-41 [21], HPA/ $\text{SiO}_2$  [22], and Preyssler type heteropoly acid [23] has been reported recently.

Dihydropyrimidone (DHPMs) derivatives have exhibited biological activities as calcium channel blockers [24], antihypertensive agents [25],  $\alpha_1$ -antagonists [26] and neuropeptide Y antagonists [27]. A broad range of biological effects including antiviral, antitumor, antibacterial and anti-inflammatory activities have been described for these compounds [28] exhibiting significant activity against HIV in AIDS therapy [29].

\* Corresponding author. E-mail: a\_teimouri@pnu.ac.ir

The initial synthesis of dihydropyrimidones following Biginelli condensations of  $\beta$ -dicarbonyl compounds with aldehydes, and urea or thiourea in the presence of catalytic amount of acid has proved to be inefficient with acidic conditions, low yields and difficult isolation, expensive reagents and environmental pollution [30]. In recent years, new methods for the synthesis of DHPM derivatives has been reported through condensation reactions between an aldehyde,  $\beta$ -keto ester and urea using  $\text{InBr}_3$  [31], silica-supported [32], microwave-assisted [33], poly(ethylene glycol) (PS-PEG) resin [34],  $\text{Yb}(\text{PFO})_3$  [35], silica immobilized nickel complex [36], heteropoly acid supported on zeolite [37], hydrotalcite [38], chitosan [39], zeolite [40], metallophthalocyanines (MPcs) [41],  $\text{Y}(\text{NO}_3)_3 \cdot 6\text{H}_2\text{O}$  [42],  $\text{H}_3\text{PW}_{12}\text{O}_{40}$  [43], copper(II) tetrafluoroborate [44], metal hydrogen sulfates  $\text{M}(\text{HSO}_4)_n$  [45], calcium fluoride [46], aqueous medium [47],  $\text{TaBr}_5$  [48], montmorillonite KSF [49], Ziegler-Natta catalyst [50], ion exchange resin [51],  $\text{I}_2$  [52], chloroacetic acid [53],  $(\text{NH}_4)_2\text{CO}_3$  [54],  $\text{PPh}_3$  [55], aluminosilicate-AIKIT-5(10) [56] and strontium(II) nitrate [57].

In spite of a large number of methods reported for this transformation, there has been a considerable interest to explore simple, milder, rapid and high-yielding protocols by employing environment-friendly and reusable catalysts. Most of the traditional processes suffer from one or more of the following drawbacks such as strong acidic conditions, pollution, high cost, low yields of the products, requirements for long reaction time and tedious work-up procedures, need to excess amounts of the reagent and the use of toxic reagents, catalysts and / or solvents. Therefore, there is a strong demand for a highly efficient and environmentally benign method for the synthesis of these heterocycles. In the recent years, the use of nano-structured ZnO [58], nano-sulfated zirconia [59], nano- $\gamma$ -alumina [60] and nano-ZSM-5 zeolite [61] catalysts has received a considerable interest in organic synthesis. This extensive application of heterogeneous catalysts in synthetic

organic chemistry can make the synthetic process more efficient from both environmental and economic points of view [62] and used catalysts can be easily recycled.

In continuation of our ongoing research for the development of simple and efficient methods for the synthesis of various heterocyclic compounds [63], herein we report the synthesis of xanthenedione derivatives through condensation reactions between aromatic aldehydes and dimedone and the synthesis of dihydropyrimidone derivatives by a three-component coupling of  $\beta$ -keto esters, aldehyde and urea in ethanol using nano-structured ZnO, nano-sulfated zirconia (SZ), nano- $\gamma$ -alumina and nano-ZSM-5 zeolites as the catalysts.

## RESULTS AND DISCUSSION

In the reaction between aromatic aldehydes, dimedone and three-component coupling,  $\beta$ -keto esters, aldehyde and urea effect of the catalyst amount was investigated (Tables 1, 2).

To minimize the formation of byproducts and to achieve good yield of the desired product, the reaction is optimized by varying the amount of catalyst (10, 25 and 50 mg), the percentage yield of xanthenedione derivatives with 10, 25 and 50 mg of SZ as a catalyst is 94, 86 and 82%, and for dihydropyrimidone derivatives it is 92, 84 and 80%, respectively (Table 1, entries 2–4). The percentage yield of xanthenedione derivatives with 10, 25 and 50 mol% of nano-ZnO as a catalyst is 88, 94 and 80%, and for dihydropyrimidone derivatives it is 87, 90 and 80%, respectively (Table 1, entries 5–7).

For nano- $\gamma$ -alumina and nano-ZMS-5 as the catalysts, when the catalyst content was increased to 50 mg, the xanthenedione derivatives yield decreased to 78% (Table 1, entry 10) and 76% (Table 1, entry 13), respectively. A similar observation was found for dihydropyrimidone derivatives and with increase of catalyst loading their yields decreased to 80 and 78%, respectively. The same reaction when performed without a catalyst for 24 h gave no product.

Table 1. Effect of the type and amount of catalysts on the synthesis of xanthenedione and dihydropyrimidone derivatives

Entry	Catalyst	Catalyst loading	Time, min	Yield, % <sup>a</sup>	
				Xanthenedione <sup>b</sup>	Dihydropyrimidone <sup>c</sup>
1.		–	24 h	No reaction	No reaction
2.	Nano-SZ	10 (mg)	120	94	92
3.		25 (mg)	120	86	84
4.		50 (mg)	120	82	80
5.	Nano-ZnO	10 (mol%)	120	88	87
6.		25 (mol%)	120	94	90
7.		50 (mol%)	120	80	80
8.	Nano- $\gamma$ -alumina	10 (mg)	120	90	87
9.		25 (mg)	120	82	84
10.		50 (mg)	120	78	80
11.	Nano-ZMS-5	10 (mg)	120	92	90
12.		25 (mg)	120	82	86
13.		50 (mg)	120	76	78

<sup>a</sup> Yields after isolation of products.

<sup>b</sup> Reaction was performed with dimedone (2 mmol), benzaldehyde (1 mmol) in the presence of catalyst.

<sup>c</sup> Ethylacetoacetate (1 mmol), corresponding aldehyde (1 mmol), urea (1.5 mmol).

Table 2. Effect of the solvent on the reaction times and yields

Entry	Solvent	Time, min	Yield, % <sup>a</sup>	
			Xanthenedione	Dihydropyrimidone
1.	H <sub>2</sub> O	120	55	60
2.	EtOH	120	93	92
3.	MeOH	120	75	70
4.	CH <sub>3</sub> CN	120	70	75
5.	1,4-Dioxan	120	65	70
6.	THF	120	60	65

<sup>a</sup> Aromatic aldehydes and dimedone (2.0 mmol), or  $\beta$ -keto esters, aldehyde and urea (2.0 mmol) in the presence of catalyst under reflux conditions in various solvents.

In order to optimize the reaction conditions, including solvents and temperature, the reaction of aromatic aldehydes and dimedone, or three-component coupling,  $\beta$ -keto esters, aldehyde and urea was optimized by reaction time and using various solvents such as EtOH, MeOH, CH<sub>3</sub>CN, 1,4-dioxane and THF (Table 2, entries 1–6). Reaction in 1,4-dioxane and THF solvent gave low product yields even after 110 min and 130 min (Table 2, entries 5 and 6).

The best results were obtained when the reaction was carried out in ethanol under reflux for 90 min in the presence of proper amount of the catalyst (Table 2, entry 2). Therefore, ethanol was selected as the solvent for this reaction. Although

water is a desirable solvent for chemical reactions for reasons of cost, safety and environmental concerns, we found that using water in this reaction gave moderate yields of products under the reflux condition after long reaction times (Table 2, entry 1).

Encouraged by these promising results, other aromatic aldehydes have been subjected to the above-mentioned optimized conditions, and the results were listed in Table 3. Several aromatic aldehydes could be converted to the corresponding products in good to high yields over nano-crystalline solid acid catalysts. Benzaldehyde and other aromatic aldehydes containing electron-withdrawing groups (nitro or

Table 3. Acid-catalyzed synthesis of xanthenedione derivatives<sup>a</sup>

Entry	Ar	Time, min/Yield, % <sup>b</sup>				MP °C (lit.) [Ref.]
		Nano-ZnO	Nano- $\gamma$ -alumina	Nano-ZMS-5	Nano-crystalline SZ	
1. (1a)	C <sub>6</sub> H <sub>5</sub>	120/88	120/90	90/92	65/94	202–204 (204–205) [17]
2. (1b)	4-ClC <sub>6</sub> H <sub>5</sub>	100/65	110/75	80/80	60/85	228–230 (230–233) [17]
3. (1c)	4-NO <sub>2</sub> C <sub>6</sub> H <sub>5</sub>	90/72	120/78	95/85	70/90	218–220 (216–218) [17]
4. (1d)	4-OHC <sub>6</sub> H <sub>5</sub>	75/65	90/82	80/85	65/92	248–250 (249–251) [17]
5. (1e)	4-CH <sub>3</sub> C <sub>6</sub> H <sub>5</sub>	80/52	90/76	70/86	60/92	210–212 (216–217) [17]
6. (1f)	4-OCH <sub>3</sub> C <sub>6</sub> H <sub>5</sub>	90/50	90/76	75/84	60/90	240–242 (244–246) [17]

<sup>a</sup> The products were characterized by IR, <sup>1</sup>H-NMR, and mass spectroscopy.

<sup>b</sup> Isolated yields.

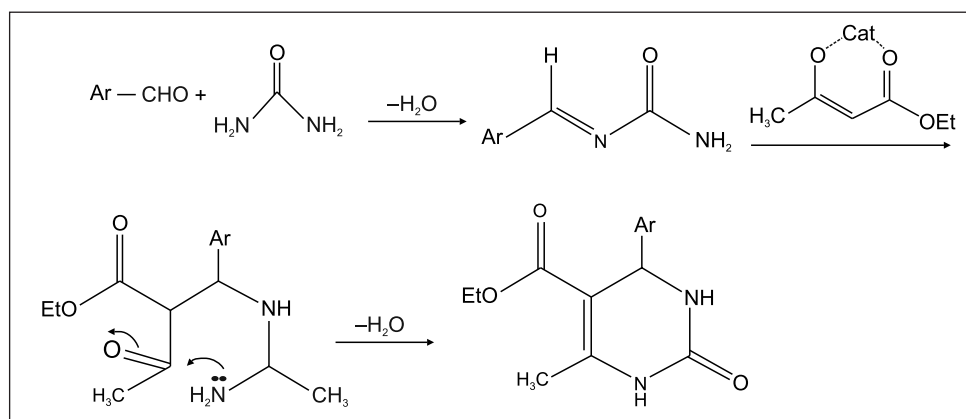


Fig. 1. Proposed mechanism for one-pot synthesis of dihydropyrimidone derivatives from benzaldehyde, ethyl acetoacetate, and urea

Table 4. Acid-catalyzed synthesis of dihydropyrimidone derivatives<sup>a</sup>

Entry	Ar	Time, min/Yield, % <sup>b</sup>				MP °C (lit.) [Ref.]
		Nano-ZnO	Nano-γ-alumina	Nano-ZMS-5	Nano-crystalline SZ	
1. (2a)	C <sub>6</sub> H <sub>5</sub>	100/88	90/87	80/90	60/92	204–206 (202–204) [27]
2. (2b)	4-ClC <sub>6</sub> H <sub>5</sub>	110/70	80/86	80/90	60/94	214–216 (212–214) [27]
3. (2c)	4-NO <sub>2</sub> C <sub>6</sub> H <sub>5</sub>	90/68	90/78	90/86	65/89	208–210 (207–209) [27]
4. (2d)	4-OHC <sub>6</sub> H <sub>5</sub>	90/62	90/75	80/80	70/93	232–234 (230–232) [27]
5. (2e)	4-CH <sub>3</sub> C <sub>6</sub> H <sub>5</sub>	80/65	75/80	80/84	50/90	214–216 (215–216) [27]
6. (2f)	4-OCH <sub>3</sub> C <sub>6</sub> H <sub>5</sub>	90/60	90/79	75/86	60/92	200–202 (201–203) [27]

<sup>a</sup> The products were characterized by IR, <sup>1</sup>H-NMR, <sup>13</sup>C-NMR and mass spectroscopy.

<sup>b</sup> Isolated yields.

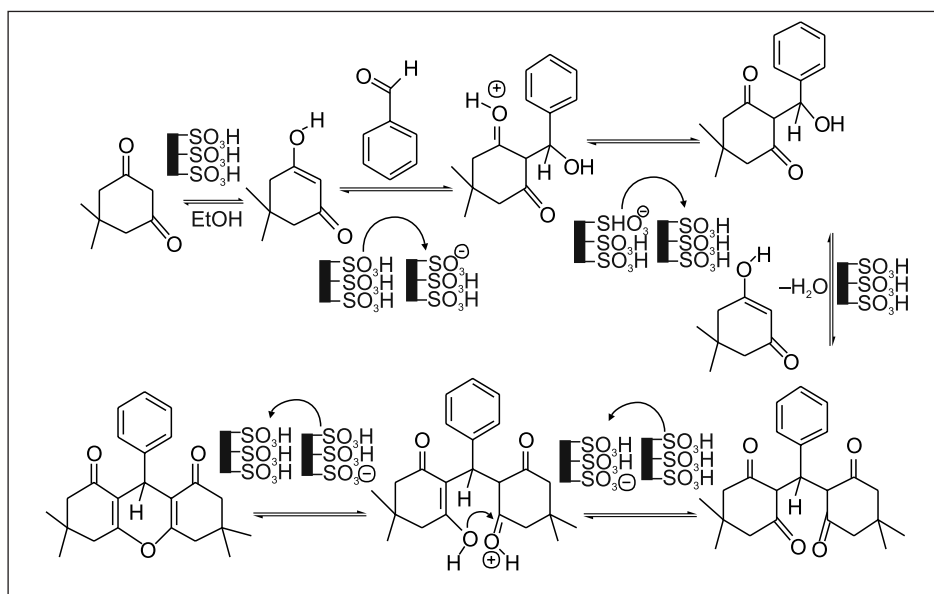


Fig. 2. Proposed mechanism for one-pot synthesis of xanthenedione derivatives

halide group) or electron-donating groups (alkyl, alkoxy or hydroxyl group) were employed and reacted well to give the corresponding xanthenediones. The reaction involves two steps to yield the expected xanthenediones: the first step is the addition step to form an intermediate, the second being the (Knoevenagel type) condensation step with the elimination of a water molecule to form the product.

Table 4 shows results of the dihydropyrimidone derivatives synthesis via the Biginelli reaction between aromatic aldehydes, 1,3-dicarbonyl compounds and urea over nano-crystalline solid acid catalysts. The presence of electron-withdrawing groups or electron-donating in the aromatic ring of the aldehydes did not have much effect on the reaction such that to afford respective products with high yields.

According to the mechanism suggested by Folkers and Johnson [64], we propose a mechanism for the formation of DHPMs 2a–f (Fig. 2). It has been hypothesized that the reaction proceeds through an acylimine intermediate and this

intermediate complex may then react with a β-ketoester. But it seems that the mechanism of Biginelli reaction is complex and further work is necessary to determine the course of the reaction.

A proposed mechanism for the role of the nano-sulfated zirconia catalyst in the reaction of benzaldehyde and dimedone is presented in Fig. 2.

Tables 5 and 6 compare the efficiency of the present method with the efficiency of other methods in the synthesis of xanthenedione and 1,4-DHPs, respectively. As evident from Tables 5 and 6, SZ shows better efficiency than other methods. In addition, the reaction times are lower than the previously reported conditions.

One of the most important advantages of heterogeneous catalysis over the homogeneous counterparts is the possibility of reusing the catalyst by simple filtration, without loss of its activity. The recovery and reusability of the catalyst was investigated in the product formation. After completion of

Table 5. Comparison of the efficiency of nano-crystalline SZ with other reported catalysts in the synthesis of xanthenedione derivatives<sup>a</sup>

Entry	Catalyst, mol%	Condition	Time	Yield, % <sup>a</sup>	References
1.	Nano-crystalline SZ	EtOH / Reflux	65 min	94	This work
2.	ZrOCl <sub>2</sub> · 8H <sub>2</sub> O	Solvent free at 80 °C	35 min	90	15
3.	20 wt% Fe <sup>3+</sup> -montmorillonite	Ethanol at 100 °C	6 h	94	18
4.	Montmorillonite-K10	Ethanol at 100 °C	6 h	60	18
5.	HPWA/MCM-41	Ethanol at 90 °C	5 h	94	21

<sup>a</sup>Benzaldehyde and dimedone in the presence of catalyst.

Table 6. Comparison of the efficiency of nano-crystalline SZ with other reported catalysts in the synthesis of dihydropyrimidone derivatives<sup>a</sup>

Entry	Catalyst, mol%	Condition	Time	Yield, % <sup>a</sup>	References
1.	Nano-crystalline SZ	EtOH / Reflux	60 min	92	This work
2.	HY Zeolite	Toluene / Reflux	12 h	64	40
3.	Montmorillonite KSF	Toluene at 100 °C	48 h	72	49
4.	Ziegler-Natta catalyst	Solvent-free 100 °C	3 h	90	50
5.	Ion exchange resin	CH <sub>3</sub> CN / Reflux	3 h	96	51
6.	Iodine as a catalyst	Toluene / Reflux	4 h	95	52
7.	Chloroacetic acid	Solvent-free 90 °C	3 h	92	53
8.	(NH <sub>4</sub> ) <sub>2</sub> CO <sub>3</sub>	H <sub>2</sub> O at 50–60 °C	4 h	92	54
9.	PPh <sub>3</sub>	Solvent-free 100 °C	10 h	70	55
10.	Aluminosilicate-AIKIT-5(10)	CH <sub>3</sub> CN / Reflux	3 h	96	56
11.	Strontium(II) nitrate	Acetic acid / Reflux	6 h	77.8	57

<sup>a</sup> Benzaldehyde, ethyl acetoacetate and urea in the presence of catalyst.

the reaction, the catalyst was separated by filtration, washed 3 times with 5 ml acetone, then several times with doubly distilled water and dried at 110 °C. Then the recovered catalyst was used in the next run. The results of three consecutive runs showed that the catalysts can be reused several times without significant loss of their activity (Fig. 3).

To illustrate efficiency of the method for preparation of 1,4-DHP's we decided to run an experiment with larger values in the optimised condition. For this purpose the reaction was repeated with 0.1 mole benzaldehyde as the selected aromatic aldehyde and appropriate reagents. The results are collected in Table 7.

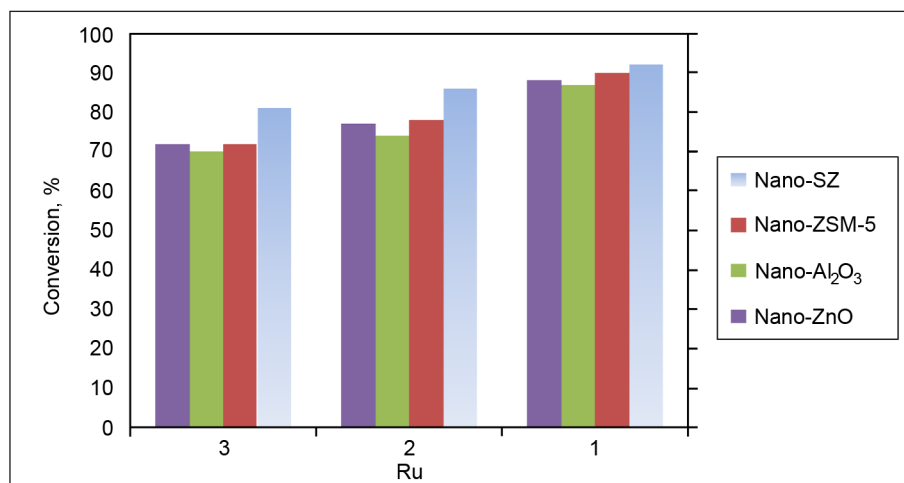


Fig. 3. The results obtained from catalyst reuse in the product formation

Table 7. Effect of reagent excess on the reaction times and yields

Entry	Catalyst	Time, h	Yield, % <sup>a</sup>
1.	Nano-SZ	4	89
2.	Nano-ZnO	4.5	86
3.	Nano-γ-alumina	7	84
4.	Nano-ZMS-5	5	87

<sup>a</sup> Benzaldehyde ethyl acetoacetate (0.1 mol) and urea (0.15 mol) in the presence of catalyst.

## EXPERIMENTAL

All reagents were purchased from Merck and Aldrich and used without further purification. Products were characterized by spectroscopy data (IR, FTIR,  $^1\text{H}$  NMR and  $^{13}\text{C}$  NMR spectra), elemental analysis (CHN) and melting points. A JASCO FT/IR-680 PLUS spectrometer was used to record IR spectra using KBr pellets. NMR spectra were recorded on a Bruker 400 Ultrashield NMR and DMSO- $d_6$  was used as a solvent. Melting points reported were determined by an open capillary method using a Galen Kamp melting point apparatus and are uncorrected. Mass Spectra were recorded on a Shimadzu Gas Chromatograph Mass Spectrometer GCMS-QP5050A/Q P5000 apparatus.

### Catalyst preparation

#### *Synthesis of nano-crystalline sulfated zirconia*

Nano-crystalline sulfated zirconia has been prepared by one step sol-gel technique [65]. A typical synthesis involves the addition of concentrated sulfuric acid (1.02 ml) to zirconium n-propoxide precursor (30 wt%) followed by the hydrolysis with water. After 3 h aging at room temperature, the resulting gel was dried at 110 °C for 12 h followed by calcination at 600 °C for 2 h.

#### *Synthesis of nano-structured ZnO*

Nano-structured ZnO has been prepared by one step sol-gel technique [66]. In a typical procedure, mixtures of ethanol, diethanolamine (DEA) and zinc acetate dihydrate were prepared. The concentration of zinc acetate dihydrate in the solvent was 0.2 M. The molar ratio of zinc acetate dihydrate and diethanolamine was 1.0. pH of the mixture was about 9. When the zinc acetate crystals were dissolved completely, sodium hydroxide (NaOH) pellets were added to the solution to increase the pH of the mixture to about 11. The resultant solution was then transferred into a Teflon-lined stainless steel autoclave which was sealed and maintained at 130 °C for 24 h.

#### *Synthesis of nano- $\gamma\text{-Al}_2\text{O}_3$ catalyst*

The nano- $\gamma\text{-Al}_2\text{O}_3$  was prepared by the sol-gel method according to the procedure described [60]. In a typical experiment, aluminum nitrate (15.614 g) was added to 400 ml of deionized water. A similar solution of sodium carbonate is prepared by dissolving (7.95 g) in 400 ml of deionized water. 200 ml of deionized water are taken in a 2 l capacity round-bottom flask and stirred well using a magnetic stirrer. Then sodium carbonate and aluminum nitrate solutions are added to 200 ml of deionized water (from separate beakers) dropwise.

The temperature was maintained 70 °C during the experiment. The pH after precipitation was found to be in the range of 7.5–8.5. The mixture was stirred for 4 h. The digested precipitates were filtered and re-dispersed again in hot 2 l of deionized water, filtered and finally washed with ethanol first

followed by acetone to avoid contamination of 'Na' ions, and air dried at room temperature. The dried precipitates were calcined in a furnace at 550 °C for 5 h to produce nano-sized  $\gamma\text{-Al}_2\text{O}_3$  powders.

#### *Synthesis of nano-ZSM-5*

For synthesis of nano-ZSM-5, tetrapropylammonium hydroxide and tetraethyl orthosilicate were the sources of aluminum and silicon, respectively. Nano-ZSM-5 zeolite was synthesized according to the procedure described earlier [67]. The components were mixed with constant stirring. After adding all the ingredients the solution was left to hydrolyze at room temperature for 48 h. The gel thus obtained was heated at 80 °C to evaporate water and ethanol formed during the reaction. The obtained solution was charged into a Teflon-lined stainless-steel autoclave under pressure and static conditions at 170 °C for 48 h. The solid phase obtained was filtered, washed with distilled water several times, dried at 120 °C and then calcined at 550 °C for 12 hours.

#### *Characterization*

X-ray diffraction patterns were recorded on a diffractometer (Philips X'pert) using CuK $\alpha$  radiation ( $\lambda = 1.5405 \text{ \AA}$ ), the crystallite size of the crystalline phase was determined from the peak of maximum intensity by using the Scherrer formula [68] with a shape factor (K) of 0.9 as below: crystallite size =  $K\lambda/W\cos\theta$ , where  $W = W_b - W_s$  and  $W_b$  is the broadened profile width of the experimental sample and  $W_s$  is the standard profile width of the reference silicon sample. FT-IR spectra of the catalysts were recorded by a FT-IR spectrophotometer in the range of 400–4000  $\text{cm}^{-1}$  with a resolution of 4  $\text{cm}^{-1}$  by mixing the sample with KBr. Specific surface area, pore volume and pore size distribution of samples calcined at 600 °C were determined from  $\text{N}_2$  adsorption-desorption isotherms at 77K (ASAP 2010 Micromeritics). The surface area was calculated by using the BET equation; pore volume and pore size distribution were calculated by the BJH method [69]. The samples were degassed under vacuum at 120 °C for 4 h, prior to adsorption measurement to evacuate the physisorbed moisture. The detailed imaging information about the morphology and surface texture of the catalyst was provided by SEM (Philips XL30 ESEM TMP), a part of the spectra data has been published in our previous work [63].

The X-ray diffraction pattern of sulfated zirconia samples, after calcination at 600 °C, showed the presence of only tetragonal phase with  $2\theta = 30.2, 50.2$  and  $60.2$  in sulfated zirconia samples.

The FT-IR-spectrum sulfated zirconia samples showed the IR bands of the  $\text{SO}_4^{2-}$  group in the region of 1240–900  $\text{cm}^{-1}$ , with peaks of the sulfate at 1238, 1145, 1072, 1043 and 996  $\text{cm}^{-1}$ , which are attributed to asymmetric and symmetric stretching frequencies S-O bond.

Figure 4 indicates the formation of crystallized alumina, as broad peaks indexed for  $\gamma\text{-Al}_2\text{O}_3$  are seen in the XRD pattern. The broadening of the XRD peaks revealed

the nano-size nature of  $\gamma$ - $\text{Al}_2\text{O}_3$  particles in alumina samples. The FT-IR spectra of alumina samples calcined at 550 °C (Fig. 5) showed an intense band centered around 3500  $\text{cm}^{-1}$  and a broad band at 1650  $\text{cm}^{-1}$ , these are assigned to stretching and bending modes of adsorbed water. The Al–O–Al bending stretching vibrations observed at around 1150  $\text{cm}^{-1}$  are due to symmetric and asymmetric bending modes, respectively. The OH torsional mode observed at 800  $\text{cm}^{-1}$  overlaps with Al–O stretching vibrations. The weak band at 2091  $\text{cm}^{-1}$  is assigned to a combination band. The bands observed at 617 and 481  $\text{cm}^{-1}$  are attributable to stretching and bending modes of  $\text{AlO}_6$  [70]. The XRD patterns of the synthesized nano-ZSM-5 show the crystallization of structures. The degree of crystallinity was determined from the peak area between  $2\theta = 20$ –24. Temperature programmed desorption of ammonia was carried out to determine the amount of acid sites relative to reference samples of zeolite with known Si/Al ratios. The XRD patterns of nano-sized ZnO particles were obtained. All nano-ZnO samples exhibited a hexagonal structure. Characteristic peaks of ZnO appeared at 31.7, 34.5, 36.2 and 56.5 (Fig. 6).

The morphology of the as prepared nano-size  $\gamma$ - $\text{Al}_2\text{O}_3$  and nano-sized ZnO powders analyzed by SEM is shown in Figs. 7–8. The SEM image demonstrates clearly the formation of spherical ZnO nanoparticles. The  $\gamma$ - $\text{Al}_2\text{O}_3$  powders indicated strong agglomeration of particles with varied spherical sizes.

#### General procedure for the synthesis of xanthenedione derivatives

In a 50 mL round bottom flask a mixture of dimedone (2 mmol) and aromatic aldehyde (1 mmol) was thoroughly mixed in ethanol (10 mL), then the catalyst was added, and the solution was refluxed for appropriate time (Table 1). The progress of the reaction was monitored by TLC. After completion of the reaction, the reaction mixture was cooled to room temperature and the resulting solid was collected by filtration and dissolved in 20 mL ethyl acetate. The catalyst was recovered by filtration. After evaporation of the solvent, the pure product could be obtained by recrystallizing in ethanol.

#### 3,3,6,6-Tetramethyl-9-(phenyl)-1,8-dioxo-1,2,3,4,5,6,7,8-octahydro-xanthene (1a)

White solid; m. p. 202–204 °C; FTIR: 2957, 1666, 1364, 1199  $\text{cm}^{-1}$ ;  $^1\text{H}$  NMR (400 MHz, DMSO- $d_6$ )  $\delta$ : 0.99 (s, 6H, 2 $\text{CH}_3$ ), 1.10 (s, 6H, 2 $\text{CH}_3$ ), 2.24 (dd,

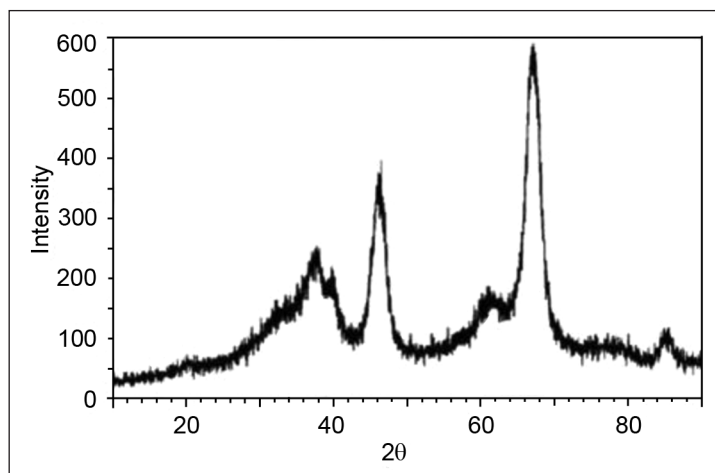


Fig. 4. XRD pattern of the nano- $\gamma$ -alumina catalyst

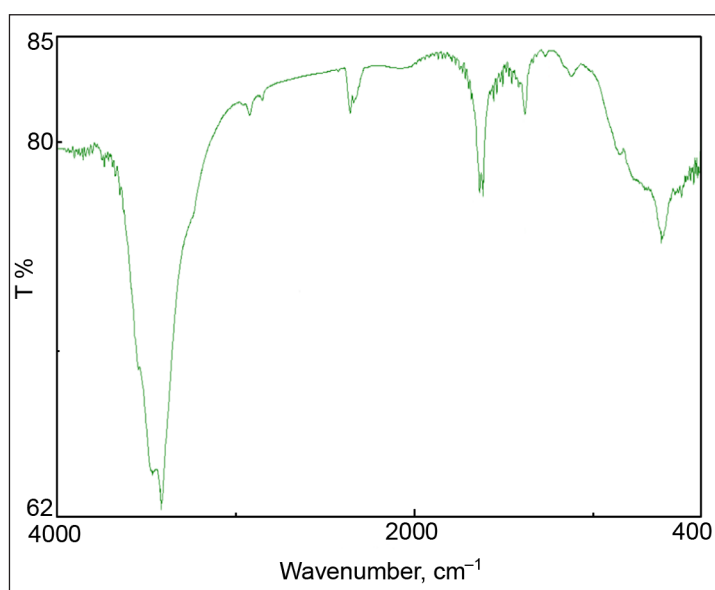


Fig. 5. FT-IR spectra of the nano- $\gamma$ -alumina catalyst

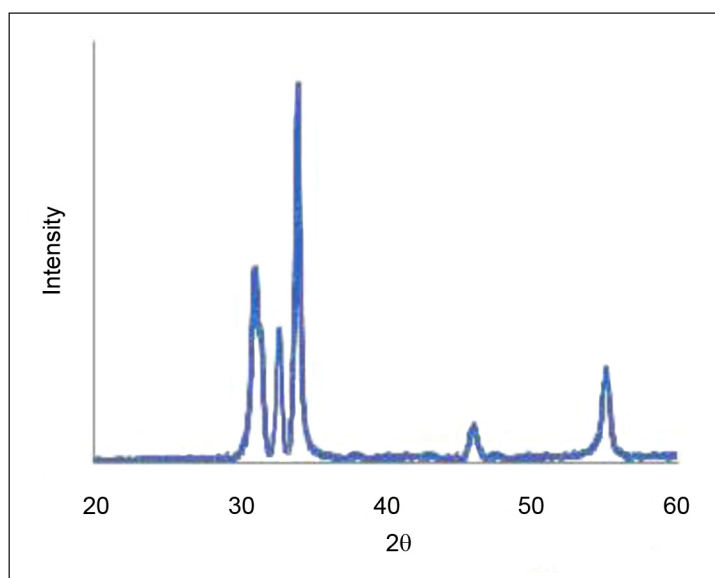


Fig. 6. XRD pattern of the nano-ZnO catalyst

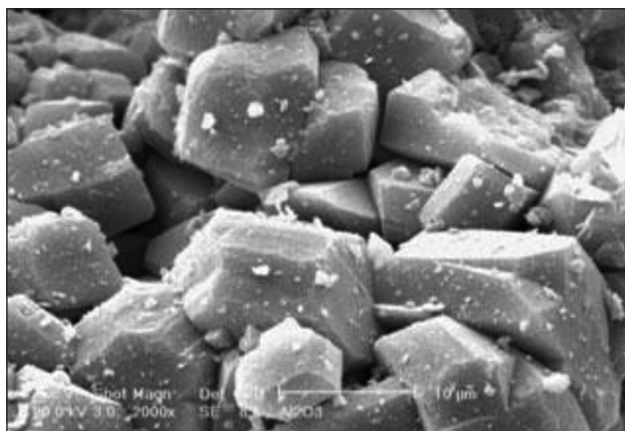


Fig. 7. SEM micrograph of the nano- $\gamma$ -alumina catalyst

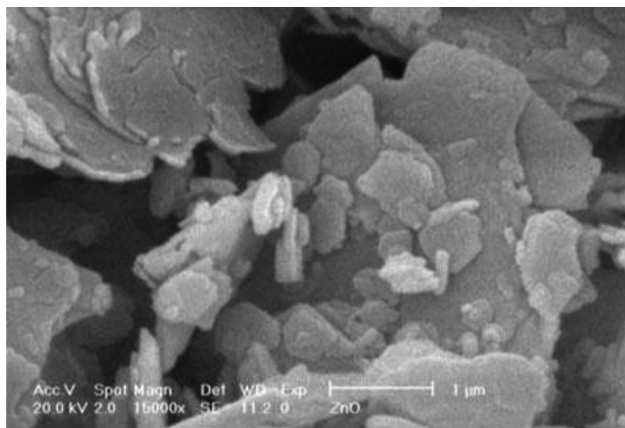


Fig. 8. SEM micrograph of the nano-ZnO catalyst

4H,  $J = 1.6$  Hz,  $J = 4.0$  Hz,  $2\text{CH}_2$ ), 2.50 (s, 4H,  $2\text{CH}_2$ ), 4.75 (s, 1H, CH), 7.10 (m, 2H, ArH), 7.20 (m, 3H, ArH);  $^{13}\text{C}$  NMR (400 MHz, DMSO- $d_6$ )  $\delta$ : 26.4, 28.2, 30.8, 31.7, 50.6, 112.1, 126.3, 127.6, 129.8, 145.1, 162.8, 195.7; Anal. calcd. for  $\text{C}_{23}\text{H}_{26}\text{O}_3$  (350.19): C, 78.83; H, 7.48. Found: C, 78.66; H, 7.32.

### 3,3,6,6-Tetramethyl-9-(4-chlorophenyl)-1,8-dioxo-1,2,3,4,5,6,7,8-octahydroxanthene (1b)

White solid; m. p. 228–230 °C; FTIR: 3 060, 2 984, 1 691, 1 666, 1 368, 1 196, 1 094  $\text{cm}^{-1}$ ;  $^1\text{H}$  NMR (400 MHz, DMSO- $d_6$ )  $\delta$ : 0.89 (s, 6H,  $2\text{CH}_3$ ), 1.12 (s, 6H,  $2\text{CH}_3$ ), 2.22 (dd, 4H,  $J = 1.6$  Hz,  $J = 2.4$  Hz,  $2\text{CH}_2$ ), 2.52 (dd, 4H,  $2\text{CH}_2$ ), 4.72 (s, 1H), 7.48–8.15 (m, 4H, ArH);  $^{13}\text{C}$  NMR (400 MHz, DMSO- $d_6$ )  $\delta$ : 26.4, 28.4, 30.6, 31.5, 50.1, 113.8, 127.3, 129.8, 130.7, 144.5, 162.6, 195.7; Anal. calcd. for  $\text{C}_{23}\text{H}_{25}\text{ClO}_3$  (384.15): C, 71.77; H 6.55. Found: C, 71.56; H 6.32.

### 3,3,6,6-Tetramethyl-9-(4-nitrophenyl)-1,8-dioxo-1,2,3,4,5,6,7,8-octahydroxanthene (1c)

White solid; m. p. 218–220 °C; FTIR: 3 082, 2 954, 1 664, 1 368, 1 170  $\text{cm}^{-1}$ ;  $^1\text{H}$  NMR (400 MHz, DMSO- $d_6$ )  $\delta$ : 0.96 (s, 6H,  $2\text{CH}_3$ ), 1.06 (s, 6H,  $2\text{CH}_3$ ), 2.12 (dd, 4H,  $J = 1.6$  Hz,  $J = 2.6$  Hz,  $2\text{CH}_2$ ), 2.50 (s, 4H,  $2\text{CH}_2$ ), 4.44 (s, 1H), 7.12–7.24 (m, 4H, ArH);  $^{13}\text{C}$  NMR (400 MHz, DMSO- $d_6$ )  $\delta$ : 26.5, 27.2, 29.3,

32.2, 50.5, 113.7, 123.5, 129.6, 146.5, 152.1, 163.6, 195.4; Anal. calcd. for  $\text{C}_{23}\text{H}_{25}\text{NO}_5$  (395.17): C, 69.86; H, 6.37. Found: C, 69.54; H, 6.12.

### 3,3,6,6-Tetramethyl-9-(4-hydroxyphenyl)-1,8-dioxo-1,2,3,4,5,6,7,8-octahydroxanthene (1d)

White solid; m. p. 248–250 °C; FTIR: 3 320, 2 956, 1 650, 1 363, 1 088  $\text{cm}^{-1}$ ;  $^1\text{H}$  NMR (400 MHz, DMSO- $d_6$ )  $\delta$ : 0.98 (s, 6H,  $2\text{CH}_3$ ), 1.14 (s, 6H,  $2\text{CH}_3$ ), 2.21 (dd, 4H,  $J = 1.6$  Hz,  $J = 2.4$  Hz,  $2\text{CH}_2$ ), 2.46 (s, 4H,  $2\text{CH}_2$ ), 4.73 (s, 1H, CH), 5.22 (s, 1H, OH), 6.70–7.12 (m, 4H, ArH);  $^{13}\text{C}$  NMR (400 MHz, DMSO- $d_6$ )  $\delta$ : 26.3, 27.5, 28.8, 32.1, 50.6, 113.4, 123.4, 146.8, 151.8, 155.2, 162.9, 195.4. m/z. 366.18 (M $^+$ ). Anal. calcd. for  $\text{C}_{23}\text{H}_{26}\text{O}_4$  (395.17): C, 75.38; H, 7.15. Found: C, 75.16; H, 6.82.

### 3,3,6,6-Tetramethyl-9-(4-methylphenyl)-1,8-dioxo-1,2,3,4,5,6,7,8-octahydroxanthene (1e)

White solid; m. p. 210–212 °C; FTIR: 3 324, 2 952, 1 662, 1 614, 1 363  $\text{cm}^{-1}$ ;  $^1\text{H}$  NMR (400 MHz, DMSO- $d_6$ )  $\delta$ : 0.98 (s, 6H,  $2\text{CH}_3$ ), 1.10 (s, 6H,  $2\text{CH}_3$ ), 2.10 (s, 3H,  $\text{CH}_3$ ), 2.22 (dd, 4H,  $J = 1.6$  Hz,  $J = 2.6$  Hz,  $2\text{CH}_2$ ), 2.44 (s, 4H,  $2\text{CH}_2$ ), 4.70 (s, 1H, CH), 6.72–7.34 (m, 4H, ArH);  $^{13}\text{C}$  NMR (400 MHz, DMSO- $d_6$ )  $\delta$ : 24.3, 26.2, 27.3, 29.1, 32.6, 50.4, 113.8, 123.2, 147.1, 151.6, 155.4, 163.1, 195.2; Anal. calcd. for  $\text{C}_{24}\text{H}_{28}\text{O}_3$  (364.2): C, 79.08; H, 7.74. Found: C, 78.86; H, 7.58.

### 3,3,6,6-Tetramethyl-9-(4-methoxyphenyl)-1,8-dioxo-1,2,3,4,5,6,7,8-octahydroxanthene (1f)

White solid; m. p. 240–242 °C; FTIR: 3 322, 2 956, 1 650, 1 616, 1 365  $\text{cm}^{-1}$ ;  $^1\text{H}$  NMR (400 MHz, DMSO- $d_6$ )  $\delta$ : 0.96 (s, 6H,  $2\text{CH}_3$ ), 1.16 (s, 6H,  $2\text{CH}_3$ ), 2.17 (s, 3H,  $\text{CH}_3$ ), 2.24 (dd, 4H,  $J = 1.6$  Hz,  $J = 2.4$  Hz,  $2\text{CH}_2$ ), 2.46 (s, 4H,  $2\text{CH}_2$ ), 4.74 (s, 1H, CH), 6.72–7.24 (m, 4H, ArH);  $^{13}\text{C}$  NMR (400 MHz, DMSO- $d_6$ )  $\delta$ : 26.6, 27.4, 29.1, 32.6, 50.6, 55.3, 113.6, 123.8, 147.3, 151.2, 157.4, 163.6, 195.4; Anal. calcd. for  $\text{C}_{24}\text{H}_{28}\text{O}_4$  (380.02): C, 75.76; H, 7.42. Found: C, 75.62; H, 6.22.

### General procedure for the synthesis of dihydropyrimidone derivatives

To a mixture of  $\beta$ -dicarbonyl compound (1 mmol), corresponding aldehyde (1 mmol), and urea (1.5 mmol) in ethanol (10 mL) the catalyst was added and the solution was refluxed for appropriate time (Table 2). After completion of the reaction as indicated by TLC, ethyl acetate was added to the solidified mixture and the insoluble catalyst was separated by filtration. After removal of the solvent, the residual solid was recrystallized from ethanol to obtain the pure product.

### 5-Ethoxycarbonyl-6-methyl-4-(phenyl)-3,4-dihydropyrimidin-2(H)-one (2a)

White solid; m. p. 204–206 °C; FTIR: 3 322, 3 165, 2 975, 1 664, 1 458, 1 358, 1 123, 1 026  $\text{cm}^{-1}$ ;  $^1\text{H}$  NMR (400 MHz, DMSO- $d_6$ )  $\delta$ : 1.16 (t, 3H,  $J = 7.2$  Hz,  $\text{CH}_3$ ), 2.32 (s, 3H,  $\text{CH}_3$ ),

4.08 (q, 2H,  $J = 7.2$  Hz,  $\text{CH}_2$ ), 5.32 (s, 1H, CH), 7.20–7.35 (m, 5H, ArH), 7.15 (s, NH), 7.74 (s, NH);  $^{13}\text{C}$  NMR (400 MHz, DMSO- $d_6$ )  $\delta$ : 14.6, 17.8, 54.6, 60.5, 94.6, 101.6, 127.2, 128.6, 129.4, 144.4, 145.6, 165.7, 174.8; Anal. calcd. for  $\text{C}_{14}\text{H}_{16}\text{N}_2\text{O}_3$  (260.12): C, 64.60, H, 6.20, N, 10.76; Found: C, 64.44, H, 6.08, N, 10.62.

#### 4-(4-Chloro-phenyl)-5-ethoxycarbonyl-6-methyl-3,4-dihydropyrimidin-2(H)-one (2b)

White solid; m. p. 214–216 °C; FTIR: 3 320, 3 164, 2 972, 1 666, 1 456, 1 352, 1 121, 1 023  $\text{cm}^{-1}$ ;  $^1\text{H}$  NMR (400 MHz, DMSO- $d_6$ )  $\delta$ : 1.12 (t, 3H,  $\text{CH}_3$ ), 2.34 (s, 3H,  $\text{CH}_3$ ), 4.02 (q, 2H,  $\text{CH}_2$ ), 5.30 (s, 1H, CH), 6.82–7.31 (dd, 4H,  $J = 8.5$  Hz, ArH), 7.14 (s, NH), 7.72 (s, NH);  $^{13}\text{C}$  NMR (400 MHz, DMSO- $d_6$ )  $\delta$ : 17.8, 50.6, 53.5, 98.7, 128.0, 128.3, 131.7, 143.5, 148.7, 151.6, 165.6; Anal. calcd. for  $\text{C}_{14}\text{H}_{15}\text{ClN}_2\text{O}_3$  (294.08): C, 57.05; H, 5.31; N, 9.50. Found: C, 56.84; H, 5.11; N, 9.42.

#### 5-Ethoxycarbonyl-6-methyl-4-(4-nitrophenyl)-3,4-dihydropyrimidin-2(H)-one (2c)

White solid; m. p. 208–210 °C; FTIR: 3 323, 3 167, 2 971, 1 668, 1 536, 1 452, 1 344, 1 127, 1 021  $\text{cm}^{-1}$ ;  $^1\text{H}$  NMR (400 MHz, DMSO- $d_6$ )  $\delta$ : 1.16 (t, 3H,  $J = 6.8$  Hz,  $\text{CH}_3$ ), 2.30 (s, 3H,  $\text{CH}_3$ ), 4.06 (q, 2H,  $J = 6.8$  Hz,  $\text{CH}_2$ ), 5.34 (s, 1H, CH), 6.91–7.34 (dd, 4H,  $J = 7.5$  Hz,  $J = 7.2$  Hz, ArH), 7.18 (s, NH), 7.70 (s, NH);  $^{13}\text{C}$  NMR (400 MHz, DMSO- $d_6$ )  $\delta$ : 14.1, 17.6, 53.9, 59.3, 99.7, 114.5, 127.2, 135.8, 146.2, 153.1, 156.7, 165.4; Anal. calcd. for  $\text{C}_{14}\text{H}_{15}\text{N}_3\text{O}_5$  (305.01): C, 55.08; H, 4.95; N 13.76. Found: C, 54.86; H, 4.71; N, 13.52.

#### 5-Ethoxycarbonyl-4-(4-hydroxyphenyl)-6-methyl-3,4-dihydropyrimidin-2(H)-one (2d)

White solid; m. p. 232–234 °C; FTIR: 3 332, 3 162, 2 976, 1 662, 1 458, 1 352, 1 126, 1 022  $\text{cm}^{-1}$ ;  $^1\text{H}$  NMR (400 MHz, DMSO- $d_6$ )  $\delta$ : 1.12 (t, 3H,  $J = 7.0$  Hz,  $\text{CH}_3$ ), 2.31 (s, 3H,  $\text{CH}_3$ ), 4.06 (q, 2H,  $J = 7.0$  Hz,  $\text{CH}_2$ ), 5.34 (s, 1H, CH), 5.26 (s, 1H, OH), 6.88–7.30 (dd, 4H,  $J = 8.4$  Hz, ArH), 7.16 (s, NH), 7.75 (s, NH);  $^{13}\text{C}$  NMR (400 MHz, DMSO- $d_6$ )  $\delta$ : 14.0, 17.7, 53.4, 59.1, 99.7, 114.8, 127.3, 135.4, 147.6, 152.4, 156.3, 165.2; Anal. calcd. for  $\text{C}_{14}\text{H}_{16}\text{N}_2\text{O}_4$  (276.41): C, 60.86; H, 5.84; N, 10.14. Found: C, 60.61; H, 5.66; N, 9.78.

#### 5-Ethoxycarbonyl-6-methyl-4-(4-methylphenyl)-3,4-dihydropyrimidin-2(H)-one (2e)

White solid; m. p. 214–216 °C; FTIR: 3 320, 3 161, 2 970, 1 665, 1 451, 1 352, 1 120, 1 026  $\text{cm}^{-1}$ ;  $^1\text{H}$  NMR (400 MHz, DMSO- $d_6$ )  $\delta$ : 1.12 (t, 3H,  $J = 7.1$  Hz,  $\text{CH}_3$ ), 2.14 (s, 3H,  $\text{CH}_3$ ), 2.34 (s, 3H,  $\text{CH}_3$ ), 4.04 (q, 2H,  $J = 7.1$  Hz,  $\text{CH}_2$ ), 5.31 (s, 1H, CH), 6.80–7.32 (dd, 4H,  $J = 8.2$  Hz, ArH), 7.16 (s, NH), 7.76 (s, NH);  $^{13}\text{C}$  NMR (400 MHz, DMSO- $d_6$ )  $\delta$ : 14.8, 18.1, 21.52, 54.6, 60.4, 101.7, 127.2, 129.8, 137.6, 141.4, 145.7, 166.3, 175.2; Anal. calcd. for  $\text{C}_{15}\text{H}_{18}\text{N}_2\text{O}_3$  (274.13): C, 65.68; H, 6.61; N, 10.21. Found: C, 65.54; H, 6.46; N, 9.82.

#### 5-Ethoxycarbonyl-4-(4-methoxyphenyl)-6-methyl-3,4-dihydropyrimidin-2(H)-one (2f)

M. p. 200–202; FTIR: 3 163, 2 971, 1 665, 1 454, 1 350, 1 121, 1 025  $\text{cm}^{-1}$ ;  $^1\text{H}$  NMR (400 MHz, DMSO- $d_6$ )  $\delta$ : 1.14 (t, 3H,  $J = 7.0$  Hz,  $\text{CH}_3$ ), 2.32 (s, 3H,  $\text{CH}_3$ ), 3.34 (s, 3H,  $\text{CH}_3$ ), 4.01 (q, 2H,  $J = 7.0$  Hz,  $\text{CH}_2$ ), 5.33 (s, 1H, CH), 6.81–7.33 (dd, 4H,  $J = 8.4$  Hz, ArH), 7.16 (s, NH), 7.76 (s, NH);  $^{13}\text{C}$  NMR (400 MHz, DMSO- $d_6$ )  $\delta$ : 14.6, 18.1, 54.2, 55.8, 60.6, 101.8, 127.4, 130.1, 137.4, 141.6, 145.7, 167.1, 175.6; Anal. calcd. for  $\text{C}_{15}\text{H}_{18}\text{N}_2\text{O}_4$  (290.13): C, 62.06; H, 6.25; N, 9.65. Found: C, 61.88; H, 5.87; N, 9.48.

## CONCLUSIONS

A one-pot, multicomponent methodology has been developed for the synthesis of xanthenedione derivatives and dihydropyrimidinone derivatives. A comparison of the catalytic efficiency of nano-sulfated zirconia, nano-structured ZnO, nano- $\gamma$ -alumina and nano-ZSM-5 zeolites with the nano-sulfated zirconia exhibiting greater activity has also been demonstrated. Compared to previously reported methods, moreover, mild reaction conditions, easy work-up, clean reaction profiles, lower catalyst loading and cost efficiency render this approach as an interesting alternative to the existing methods.

## ACKNOWLEDGEMENTS

Supports from the Payame Noor University in Isfahan Research Council and helps of the Isfahan University of Technology are gratefully acknowledged. Thanks are also due to Mrs. Shahraki and Mr Narimani for recording the FT-IR spectra of the compound.

Received 22 March 2013

Accepted 20 May 2013

## References

1. H. K. Wang, S. L. Morris-Natschke, K. H. Lee, *Med. Res. Rev.*, **17**, 367 (1997).
2. A. V. Rakavishnikov, M. P. Smith, B. Birrell, J. F. W. Gkeana, O. H. Griffith, *Tetrahedron Lett.*, **39**, 6637 (1998).
3. P. Poupelin, G. Saint-Rut, O. Fussard-Blanpin, G. Narcisse, G. Uchida-Ernouf, R. Lakroix, *Eur. J. Med. Chem.*, **13**, 67 (1978).
4. R. W. Lambert, J. A. Martin, J. H. Merrett, K. E. B. Parkes, G. J. Thomas, PCT Int. Appl. WO 9706178, 1997.
5. E. S. H. El Ashry, L. F. Awada, E. S. I. Ibrahim, O. K. Bdeewy, *Arkivoc*, **ii**, 178 (2006).
6. K. Chibale, M. Visser, D. V. Schalkwyk, P. J. Smith, A. Saravanamuthu, A. H. Fairlamb, *Tetrahedron*, **59**, 2289 (2003).
7. S. Hatakeyma, N. Ochi, H. Numata, S. Takano, *J. Chem. Soc., Chem. Commun.*, **17**, 1202 (1988).

8. J. Kuthan, P. Sebek, S. Bohm, *Advances in Heterocyclic Chemistry*, Vol. 62, Academic Press, Inc., New York (1995).
9. N. Rashed, M. Sayed, E. S. H. El Ashry, *J. Chin. Chem. Soc.*, **40**, 189 (1993).
10. D. Q. Shi, Q. Y. Zhuang, *Chinese J. Org. Chem.*, **23**, 694 (2003).
11. B. Das, P. Thirupathi, K. R. Reddy, B. Ravikanth, L. Nagarapu, *Catal. Commun.*, **8**, 535 (2007).
12. T. S. Jin, J. S. Zhang, A. Q. Wang, T. S. Li, *Synth. Commun.*, **35**, 2339 (2005).
13. G. Imani-Shakibaei, P. Mirzaei, A. Bazgir, *Appl. Catal. A.*, **325**, 188 (2007).
14. M. Seyyedhamzeh, P. Mirzaei, A. Bazgir, *Dyes Pigm.*, **76**, 836 (2008).
15. E. Mosaddegh, M. R. Islami, A. Hassankhani, *Arabian J. Chem.*, **5**, 77 (2012).
16. X. Fan, X. Hu, X. Zhang, J. Wang, *Can. J. Chem.*, **83**, 16 (2005).
17. X. S. Fan, Y. Zhen, X. Y. Zhang, X. Y. Hu, J. J. Wang, *Chin. Chem. Lett.*, **16**(7), 897 (2005).
18. G. Song, B. Wang, H. Luo, L. Yang, *Catal. Commun.*, **8**, 673 (2007).
19. A. Pramanik, S. Bhar, *Catal. Commun.*, **20**, 17 (2012).
20. B. Das, P. Thirupathi, I. Mahender, V. S. Reddy, Y. K. Rao, *J. Mol. Catal. A: Chem.*, **247**, 233 (2006).
21. G. Karthikeyan, A. Pandurangan, *J. Mol. Catal. A: Chem.*, **311**, 36 (2009).
22. M. M. Amini, M. Seyyedhamzeh, A. Bazgir, *Appl. Catal. A.*, **323**, 242 (2007).
23. M. M. Heravi, K. Bakhtiari, Z. Daroogheha, F. F. Bamoharram, *J. Mol. Catal. A: Chem.*, **273**, 99 (2007).
24. C. O. Kappe, *Eur. J. Med. Chem.*, **35**, 1043 (2000).
25. K. S. Atwal, B. N. Swanson, S. E. Unger, et al., *J. Med. Chem.*, **34**, 806 (1991).
26. C. O. Kappe, W. M. F. Fabian, M. A. Semones, *Tetrahedron*, **753**, 2803 (1999).
27. M. A. Bruce, G. S. Pointdexter, G. Johnson, PCT Int. Appl. WO 98 33791, 1998.
28. C. O. Kappe, O. V. Shishkin, G. Uray, P. Verdino, *Tetrahedron*, **56**, 1859 (2000).
29. P. A. Evans, T. Manangan, *Tetrahedron Lett.*, **46**, 8811 (2005).
30. Y. Ma, C. Qian, L. Wang, M. Yang, *J. Org. Chem.*, **65**, 3864 (2000).
31. N. Y. Fu, Y. F. Yuan, Z. Cao, S. W. Wang, J. T. Wang, C. Peppe, *Tetrahedron*, **58**, 4801 (2002).
32. K. Niknam, A. Hasaninejad, M. Arman, *Chin. Chem. Lett.*, **21**, 399 (2010).
33. H. Khabazzadeh, K. Saidi, H. Sheibani, *Bioorg. Med. Chem. Lett.*, **18**, 278 (2008).
34. Z.-J. Quan, Y.-X. Da, Z. Zhang, X.-C. Wang, *Catal. Commun.*, **10**, 1146 (2009).
35. M. Wu, J. Yu, W. Zhao, J. Wu, S. Cao, *J. Fluorine Chem.*, **132**, 155 (2011).
36. R. K. Sharma, D. Rawat, *Inorg. Chem. Commun.*, **17**, 58 (2012).
37. M. Moosavifar, *C. R. Chim.*, **15**, 444 (2012).
38. J. Lal, M. Sharma, S. Gupta, P. Parashar, P. Sahu, D. D. Agarwal, *J. Mol. Catal. A: Chem.*, **352**, 31 (2012).
39. J. Lal, S. K. Gupta, D. D. Agarwal, *Catal. Commun.*, **27**, 38 (2012).
40. M. Tajbakhsh, B. Mohajerani, M. M. Heravi, A. N. Ahmadi, *J. Mol. Catal. A: Chem.*, **236**, 216 (2005).
41. S. L. Jain, J. K. Joseph, S. Singhal, B. Sain, *J. Mol. Catal. A: Chem.*, **268**, 134 (2007).
42. N. S. Nandurkar, M. J. Bhanushali, M. D. Bhor, B. M. Bhanag, *J. Mol. Catal. A: Chem.*, **271**, 14 (2007).
43. B. G. Mishra, D. Kumar, V. S. Rao, *Catal. Commun.*, **7**, 457 (2006).
44. A. Kamal, T. Krishnaji, M. A. Azhar, *Catal. Commun.*, **8**, 1929 (2007).
45. K. Niknam, M. A. Zolfigol, Z. Hossiennejad, N. Daneshvar, *Chin. J. Catal.*, **28**(7), 591 (2007).
46. S. Chitra, K. Pandiarajan, *Tetrahedron Lett.*, **50**, 2222 (2009).
47. P. G. Mandhane, R. S. Joshi, D. R. Nagargoje, C. H. Gill, *Tetrahedron Lett.*, **51**, 3138 (2010).
48. N. Ahmed, J. E. van Lier, *Tetrahedron Lett.*, **48**, 5407 (2007).
49. F. Bigi, S. Carloni, B. Frullanti, R. Maggi, G. Sartori, *Tetrahedron Lett.*, **40**, 3465 (1999).
50. A. Kumar, R. A. Maurya, *J. Mol. Catal. A: Chem.*, **272**, 53 (2007).
51. J. K. Joseph, S. L. Jain, B. Sain, *J. Mol. Catal. A: Chem.*, **247**, 99 (2006).
52. R. S. Bhosale, S. V. Bhosale, S. V. Bhosale, T. Wang, P. K. Zubaidda, *Tetrahedron Lett.*, **45**, 9111 (2004).
53. Y. Yu, D. Liu, C. Liu, G. Luo, *Bioorg. Med. Chem. Lett.*, **17**, 3508 (2007).
54. F. Tamaddon, Z. Razmi, A. A. Jafari, *Tetrahedron Lett.*, **51**, 1187 (2010).
55. A. Debache, M. Amimour, A. Belfaitah, S. Rhouati, B. Carboni, *Tetrahedron Lett.*, **49**, 6119 (2008).
56. D. Shobha, M. A. Chari, A. Mano, S. T. Selvan, K. Mukkanti, A. Vinu, *Tetrahedron*, **65**, 10608 (2009).
57. C. Liu, J. Wang, Y. Li, *J. Mol. Catal. A: Chem.*, **258**, 367 (2006).
58. S. K. Asl, S. K. Sadrnezhad, M. Kianpour-Rad, *Mater. Lett.*, **64**, 1935 (2010).
59. B. Tsyntsarski, V. Avreyska, H. Kolev, T. Marinova, D. Klisurski, K. Hadjiivanov, *J. Mol. Catal. A: Chem.*, **193**, 139 (2003).
60. K. M. Parida, A. C. Pradhan, J. Das, N. Sahu, *Mater. Chem. Phys.*, **113**, 244 (2009).
61. N. Viswanadham, S. K. Saxena, M. Kumar, *Pet. Sci. Technol.*, **29**, 393 (2011).
62. G. Santor, R. Maryi, P. Righi, *Chem. Ber.*, **104**, 199 (2004).
63. A. Teimouri, A. N. Chermahini, *J. Mol. Catal. A: Chem.*, **346**, 39 (2011).
64. K. Folkers, H. J. Harwood, T. B. Johnson, *J. Am. Chem. Soc.*, **54**, 3751 (1932).
65. M. K. Mishra, B. Tyagi, R. V. Jasra, *J. Mol. Catal. A: Chem.*, **223**, 61 (2004).
66. K. J. Chen, F. Y. Hung, S. J. Chang, S. J. Young, Z. S. Hu, *Curr. Appl. Phys.*, **11**, 1243 (2011).

67. M. Firoozi, M. Baghalha, M. Asadi, *Catal. Commun.*, **10**, 1582 (2009).
68. B. D. Cullity, S. R. Stock, *Elements of X-ray Diffraction*, 3rd edn., Prentice Hall, Upper Saddle River, NJ (2001).
69. S. J. Gregg, S. W. Sing, *Adsorption, Surface Area and Porosity*, 2nd edn., Academic Press, New York (1982).
70. P. H. Colombari, *J. Mater. Sci. Lett.*, **7**, 1324 (1988).

Abbas Teimouri, Alireza Najafi Chermahini, Leila Ghorbanian

**KSANTENEDIONO IR DIHIDROPIRIMIDONO  
DARINIŲ ŽALIOJI SINTEZĖ, KATALIZUOJAMA  
NANOKRISTALINIAIS KIETAISIAIS RŪGŠTINIAIS  
KATALIZATORIAIS**

*S a n t r a u k a*

Aprašyta paprasta universali ksantenediono ir dihidropirimidono darinių sintezė kondensacijos reakcijų pagalba, katalizatoriais naudojant nanostruktūrizuotus cirkonio, cinko, aliuminio oksidus bei nano-ZSM-5 ceolitus.